ORIGINAL RESEARCH

Combined 3T Diffusion Tensor Tractography and ^{1}H-MR Spectroscopy in Motor Neuron Disease

M. Nelles
W. Block
F. Träber
U. Wüllner
H.H. Schild
H. Urbach

BACKGROUND AND PURPOSE: Diagnostic confidence in motor neuron disease may be improved by the use of advanced MR imaging techniques. Our aim was to assess the accuracy (sensitivity/specificity) and agreement of combined ^{1}H-MR spectroscopy (proton MR spectroscopy) and diffusion tensor imaging (DTI) at 3T in patients with suspected motor neuron disease regarding detection of upper motor neuron (UMN) dysfunction.

MATERIALS AND METHODS: Eighteen patients with suspected motor neuron disease were studied with MR spectroscopy/DTI and clinically rated according to the El-Escorial and ALSFRS-R scales. For MR spectroscopy, absolute *N*-acetylaspartate (NAA), choline (Cho), and phosphocreatine (PCr) concentrations and relative NAA/Cho and NAA/PCr ratios of corresponding volumes of interest within the primary motor cortex were calculated. For DTI, fractional anisotropy (FA) and mean diffusivity (MD) were measured bilaterally at the level of the precentral gyrus, corona radiata, internal capsule, cerebral peduncles, pons, and pyramid. FA and MD statistics were averaged on the corticospinal tracts (CSTs) as a whole to account for a region-independent analysis.

RESULTS: MR spectroscopy indicated NAA reduction beyond the double SD of controls in 6 of 8 patients with clinical evidence for UMN involvement. Congruently, the mean FA of these patients was significantly lower in the upper 3 regions of measurements ($P < .01$). Overall, MR spectroscopy and DTI were concordant in all except 3 cases: 1 was correctly excluded from motor neuron disease by DTI (genetically proved Kennedy syndrome), whereas MR spectroscopy indicated CST involvement. MR spectroscopy and DTI each were false-positive for CST affection in 1 patient with lower motor neuron involvement only.

CONCLUSION: Combined MR spectroscopy/DTI at 3T effectively adds to the detection of motor neuron disease with a high degree of accordance.

Amyotrophic lateral sclerosis (ALS), Lou Gehrig syndrome or Charcot disease, is the most common progressive motor neuron disease.[1] Classic ALS affects the upper (UMN) and lower motor neurons (LMN), but cases with predominant UMN or LMN involvement also occur. It is still debated whether primary lateral sclerosis (PLS) and ALS are distinct disorders or manifestations of a single disorder, and a classification into ALS, UMN– dominant ALS, and PLS has been proposed to systematize future trials,[2] hence the correctness of UMN assessment is crucial.

In addition to traditional diagnostic steps, such as electromyography, transcranial magnetic stimulation,[3,4] and assessment according to established clinical rating scales (eg, El-Escorial [EE][5] or ALS Functional Rating Scale-Revised [ALSFRS-R[6]]), recent promising attempts to improve diagnostic confidence of UMN assessment used advanced MR imaging techniques: ^{1}H-MR spectroscopy (proton MR spectroscopy),[7-11] diffusion tensor imaging (DTI),[12-19] diffusion tensor tractography (DTT),[20] or combinations thereof.[21,22] However, systematic evaluation of their concordance in the same patients is still rare.[21,23]

To obtain a definite diagnosis early in the disease is important for therapeutic intervention,[21,24] quality of life,[17,25,26] and monitoring therapeutic trials.[16,22] Cervical myelopathy, Kennedy syndrome (spinobulbar muscle atrophy, [SBMA]), peripheral nerve lesions, and multifocal polyneuropathy are, among others, differential diagnoses that have to be excluded. The clinical diagnosis is especially difficult when UMN involvement remains unclear. The previously mentioned techniques not only hold the promise of a more specific and potentially objective MR imaging measure but may even lead to a biomarker of disease severity.

In contrast, most characteristics observed on structural MR imaging, such as corticospinal tract (CST) hyperintensities in T2-weighted, proton density, and fluid-attenuated inversion recovery (FLAIR) imaging[27-32]; hypointense precentral gyrus changes[33,34]; or marked frontal or callosal atrophy,[35] are rather uncertain.[31,32] CST hyperintensities are frequently found in healthy individuals, whereas the hypointense precentral gyrus sign apparently is motor neuron disease–specific according to Ishikawa et al[33] but occurs only in a minority of patients with ALS. To our knowledge, none of these signs have yet been studied at 3T. The principal aim of the present study was to evaluate the diagnostic accuracy of combined MR spectroscopy and DTI at 3T as an additional diagnostic tool in patients with suspected motor neuron disease and to provide an estimate of their concordance when applied to the same patients.

Materials and Methods

Healthy Controls and Patients

Study participants comprised 2 separate groups of healthy controls (20 for MR spectroscopy: 13 men; mean age, 51 years; range, 30–74 years; 34 for DTI: 17 men; mean age, 53 years; range, 33–79 years) and 18 patients with suggested motor neuron disease (11 men; mean age,

Received March 9, 2008; accepted after revision May 10.

From the Departments of Radiology (M.N., W.B., F.T., H.H.S., H.U.) and Neurology (U.W.), University of Bonn Medical Center, Bonn, Germany.

Please address correspondence to Michael Nelles, MD, Department of Radiology/Neuroradiology, University of Bonn Medical Center, Sigmund Freud Str 25, D-53105 Bonn, Germany; e-mail: michael.nelles@ukb.uni-bonn.de

DOI 10.3174/ajnr.A1201

59 years; range, 45–73 years). The control samples were acquired independently in preceding investigations by using the same MR imaging equipment and techniques as in the actual patient study. The overall group of patients consisted of patients admitted consecutively to our Neuromuscular Clinic for suspected motor neuron disease. Mean disease duration (symptom onset to time of MR spectroscopy/DTI) was 20 ± 9 months. Neurologic rating was based on the EE and ALSFRS-R scales and was conducted by an experienced neurologist (U.W.). On rigorous examination, patients were grouped according to the EE scale; ALSFRS-R served to further assess disease severity. Group I was composed of the healthy controls; group II comprised 4 patients who did not meet EE criteria; group III, 7 individuals with "clinically possible" assessments; and group IV, 7 patients with clinical evidence for UMN involvement (4 "definite" and 3 "clinically probable" patients). No patients with familial ALS were included in this study.

MR Imaging

All of the MR imaging data were acquired on a 3T Achieva MR imaging system (Philips Medical Systems, Best, the Netherlands). Routine imaging pulse sequences included axial T2-weighted turbo spin-echo (TSE) scans (TR, 4000 ms; TE, 80 ms, TSE factor, 15; section thickness, 5 mm), isotropic FLAIR imaging (TR, 12000 ms; TE, 140 ms, TSE factor, 40; section thickness, 2 mm; section gap, 0 mm; voxel dimensions, $2 \times 2 \times 2$ mm^3), and additional coronal T2-weighted planscans (TR, 4752 ms; TE, 80 ms; section thickness, 4 mm) for targeting the spectroscopic voxel (volume of interest [VOI]). The geometry of the FLAIR sequences was identical to the DTI dataset parameters detailed below; DTI/FLAIR overlays were used as an anatomic reference frame for a guided placement of tracking seeds during tractography. Furthermore, 2 observers independently read all anatomic images regarding occurrence of 1) CST hyperintensities on FLAIR images, and 2) the hypointense precentral gyrus sign in T2-weighted and/or FLAIR sequences.

MR Spectroscopy

For MR spectroscopy, bilateral $30 \times 25 \times 20$ mm^3 VOIs were placed anterior to the central sulcus (Fig 1*A*). VOI positioning was done semiautomatically by the manufacturer-supplied "SmartPlan" algorithm[36] and was then controlled and confirmed by an experienced scientist in each individual investigation. Spectra-acquisition parameters by using the point-resolved spectroscopy technique were as follows: with water (H_2O)-suppression: 1) TR/TE, 2000/140 ms (96 averages); without H_2O-suppression: 2) TR/TE 3500/140 ms (32 averages) and 3) TR/TE 6000/30, 60, 100, 140, 280, 500, 800 ms (4 averages). Postprocessing and quantification of all spectra were performed with the Java-MRUI software package[37] by using time-domain analysis by the advanced method for accurate, robust, and efficient spectral fitting (AMARES) algorithm.[38] Subsequently, the absolute concentration of *N*-acetylaspartate (NAA) in brain tissue was determined by referencing the NAA signal intensity to the internal H_2O signal intensity in the unsuppressed acquisition with TE 140 ms and extrapolating to TE 0 and TR ∞ (by using metabolite relaxation times taken from Träber et al[39]). The T2 of H_2O in brain tissue and in CSF and the correction for partial CSF volume within the VOI were obtained from a biexponential fit to the unsuppressed series with 7 TE values.

Finally, absolute concentrations of choline (Cho) and phosphocreatine (PCr) and relative metabolite ratios NAA/Cho and NAA/PCr were calculated from the H_2O-suppressed acquisition with TE 140 ms, with the concentrations corrected for partial CSF volume referring to brain tissue contents within the VOI (thus not being influenced by higher CSF volume in the VOI due to brain atrophy). Total MR spectroscopy scanning time was 20 minutes for all acquisitions from both VOIs, including spectral preparations.

DTI

For DTI, a sensitivity encoding[40] (SENSE) spin-echo echo-planar imaging (SENSE factor 2.2) pulse sequence with scanning parameters as noted was applied (TE, 54 ms; TR, 5807 ms; voxel dimensions, $2 \times 2 \times 2$ mm^3; sections, 60; FOV, 256; reconstruction matrix, 128×128; gradient directions, 16; b-value, 600 s/mm^2 [2 acquisitions]). Acquisition time for this protocol was 3:24 minutes. Tractographies followed the fiber tracking approach proposed by Mori et al and Stieltjes et al.[41-43] Seed regions were placed in the pons, posterior limb of the internal capsule, and the centrum semiovale. Line-propagation thresholds to terminate the tracking process were ≤0.15 for fractional anisotropy (FA) and ≥27° as an angle threshold, respectively. On the basis of the 3D CST tractographies, 2D FA overlay maps on which the corticospinal tract could be easily identified were generated throughout the whole brain (Fig 1*B*), allowing a more unbiased determination of diffusion characteristics along the CSTs, as shown by Wang et al,[21] compared with manual unguided region-of-interest placement. Furthermore, the DTI atlas project by Wakana et al[44] was used as an additional anatomic framework.

FA and mean diffusivity (MD) were measured bilaterally at the level of the pyramid, pons, cerebral peduncles, internal capsule, corona radiata, and precentral gyrus (Fig 1*B*). The region-of-interest size was 4×4 voxels, thus covering an area of 64 mm^2 in both hemispheres at every measurement level. Region-of-interest placement was done in noninterpolated images to minimize partial volume effects possibly induced by CSF and structures adjacent to the CST (such as the basal ganglia). Region-of-interest independent fiber tract analysis was performed in a volumetric approach that calculated the number of voxels of which CSTs were composed and their diffusion characteristics (FA, MD) along the whole fiber "object." Observers were blinded to results of clinical ratings. MR spectroscopy and DTI were evaluated independently by different investigators.

Follow-Up Examinations

The clinical course could be monitored in 6 equivocal cases (patients III/2-III/7, Table 1) and in 12 patients overall (IV/3-IV/6, III/1-III/7, II/2; Table 1). MR imaging follow-up examinations were performed in 3 patients without clear UMN signs with a mean interval of 168 days (III/4, III/6, II/2; Table 1).

Statistics

For statistical analyses, the mean values for the right and left hemispheres were calculated and used in the analysis. FA values were scaled by a factor of 1000. Nonparametric Mann-Whitney–Wilcoxon tests were used to check for equality of means between different subgroups. Single results for MR spectroscopy and DTI were assumed to be pathologic when they were below the double SDs of healthy controls (in 2 or more adjacent regions regarding the FA and MD measurements). For post hoc determination of combined MR spectroscopy/DTI sensitivity and specificity, the clinical evidence for UMN involvement served as a ground truth on the basis of which the correctness of combined results was rated. An overall negative result was presumed in the case of divergent or negative findings in both

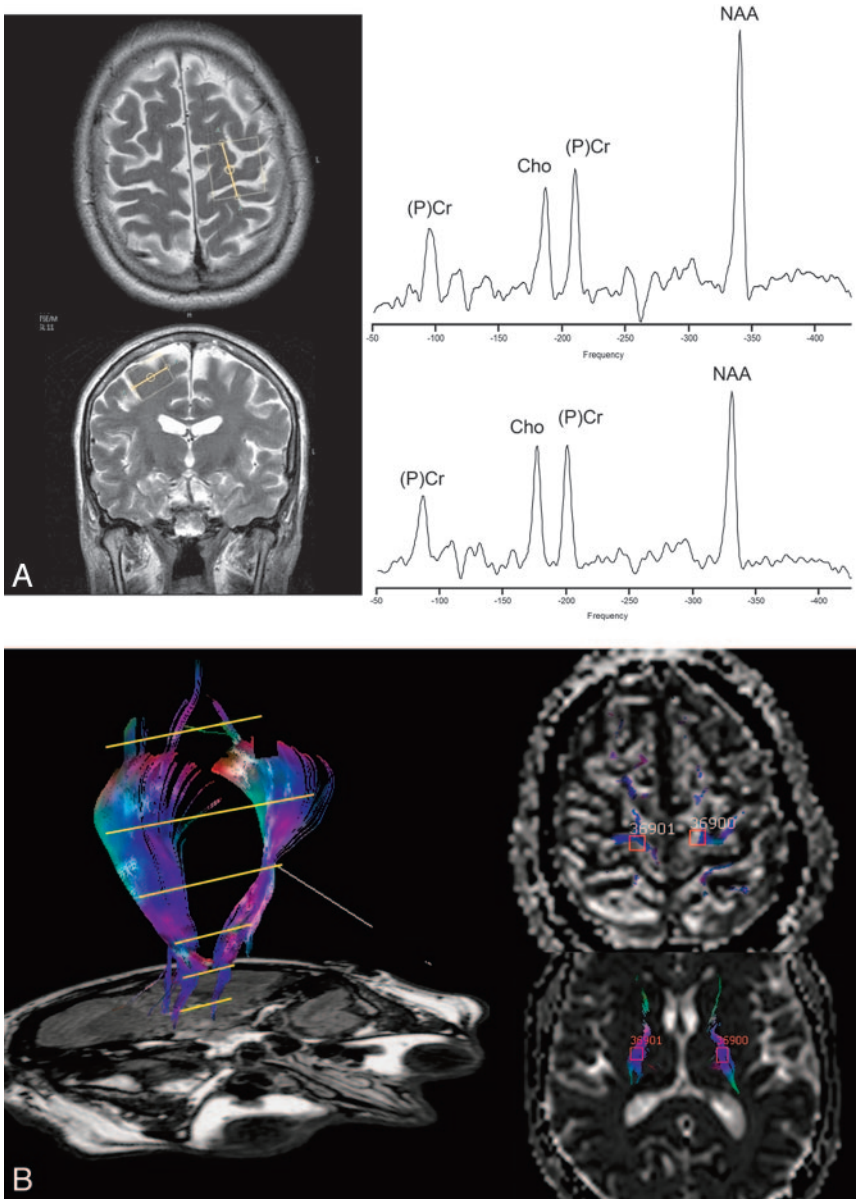

Fig 1. *A*, Illustration of spectroscopic VOI in the central region in axial (left hemisphere) and coronal (right hemisphere) T2-weighted planscan images (left, upper and lower row). Sample spectra (TR/TE, 2000/140 ms; H_2O-suppressed) of a healthy control (right, upper row) and patient IV/7 (Table 1) (right, lower row). *B*, 3D DTT (left) with intersection lines (yellow) shown at the level of FA/MD measurements (precentral gyrus, corona radiata, internal capsule, cerebral peduncles, pons, and pyramid). Fibers are projected onto axial FA (right/upper row, precentral gyrus) and MD maps (right/lower row, internal capsule) to allow a guided region-of-interest placement along the corticospinal tract. FA and MD statistics were additionally averaged on the CSTs as a whole to account for a region-independent analysis.

techniques; reduction beyond the single SD threshold for MR spectroscopy and beyond the double SD threshold in only 1 region for DTI was regarded as a pathologic result of the MR spectroscopy/DTI combination.

Results

Patients

The ALSFRS-R scores of the 18 patients declined over the subgroups: group II conformed more closely to the maximum score of 48 (ie, 36), whereas groups III and IV were nearly even at a score below 30 (ie, 28 and 29, respectively). The mean degree of impairment (ALSFRS-R) was 30 ± 5. Group II (criteria not met) motor neuron disease differential diagnoses were cervical myelopathy (II/1, Table 1), polyneuropathy (II/2), SBMA (II/3), and suggested spinal muscle atrophy (II/4).

Structural 3T MR Imaging

Anatomic MR imaging signs as described previously (ie, concurrent/simultaneous occurrence of both the hypointense cortical band and CST signal-intensity changes) were present in 3 of the 7 group IV (EE "probable/definite") patients (IV/1, IV/4, IV/7) and in neither of the healthy controls. Overall, they were observed in a total of 5 patients (IV/1, IV/4, IV/7, III/7, II/1), with both signs present simultaneously in all except 1 patient who belonged to the clinically possible group and in whom CST signal intensity elevation was absent (III/7). Most interesting, both criteria were present in a patient with severe

Table 1: Results of the combination MR Spectroscopy/DTI*

Patient No.	UMN†	MRS	DTI	MRS/DTI	TMS‡	DENERV§
Group IV						
1	+	++	++	true pos.	NA	+
2	+	+	+	true pos.	–	+
3	+	++	++	true pos.	–	–
4	+	++	++	true pos.	+	–
5	+	++	++	true pos.	+	+
6	+	+	+	true pos.	–	+
7	+	++	++	true pos.	+	+
Group III						
1	+	++	++	true pos.	+	–
2	–	++	++	false pos.	NA	+
3	–	–	–	true neg.	–	–
4	–	–	–	true neg.	+	+
5	–	+	–	true neg.	–	+
6	–	–	–	true neg.	+	+
7	–	–	+	true neg.	NA	+
Group II						
1	–	–	–	true neg.	+	–
2	–	–	–	true neg.	–	–
3	–	++	–	true neg.	–	+
4	–	–	–	true neg.	–	–

Note:—MRS indicates MR spectroscopy; UMN, upper motor neuron; TMS, transcranial magnetic stimulation; DENERV, denervation; true pos., true-positive; false pos., false positive; true neg., true negative; NA, not applicable; DTI, diffusion tensor imaging.
* ++ for MRS indicates NAA/Cho reduction beyond double SD; + beyond single SD. For DTI, ++ indicates 2 or more regions with FA below double SD; + just 1 region, respectively. – indicates a negative result. Reduction beyond the single SD threshold for MRS and beyond the double SD threshold in 1 region for DTI is regarded as a pathologic result of the MRS/DTI combination; discordance is graded as negative. Note that patient III/1 had primary lateral sclerosis but was subgrouped into the "clinically possible" group (III) due to his initial EE rating. DTI and MRS concurrently are false-positive in 1 patient with lower motor neuron involvement only (patient III/2).
† Clinical evidence for upper motor neuron involvement.
‡ Pathologic central conduction times in transcranial magnetic stimulation.
§ Presence or absence of generalized denervation.

Table 2: NAA/Cho and NAA/PCr metabolite ratios and absolute molar concentrations of NAA, Cho, and PCr (mmol/L brain tissue, mM) for patient subgroups and healthy controls (group Ia)

Group	NAA/Cho	NAA/PCr	NAA (mM)	Cho (mM)	PCr (mM)
IV* mean	1.72	1.62	9.79	1.88	8.19
SD	0.20	0.11	0.70	0.21	0.70
III mean	2.08	1.83	10.36	1.64	7.61
SD	0.36	0.18	1.92	0.21	1.03
II mean	2.10	1.78	10.26	1.60	7.78
SD	0.25	0.09	1.77	0.23	1.16
Ia mean	2.11	1.82	12.64	2.00	9.15
SD	0.14	0.12	1.16	0.21	1.24

Note:—NAA indicates *N*-acetylaspartate; Cho, choline; PCr, phosphocreatine.
* Both metabolite ratios are lowest in group IV.

cervical myelopathy in whom motor neuron disease could be ruled out (II/1).

MR Spectroscopy

Metabolite ratios for NAA/Cho and NAA/PCr and absolute quantifications for these metabolites are detailed in Table 2. Normal ranges for NAA/Cho and NAA/PCr were 2.11 ± 0.14 and 1.82 ± 0.12, respectively. NAA/Cho was a robust parameter to enable proper differentiation of patient subgroups, showing a decline from patients who did not meet EE criteria (mean ratio, 2.10 ± 0.25) toward the probable/definite group (1.72 ± 0.20, $P < .05$, Fig 2*A*). Both parameters were lowest in group IV (EE probable/definite).

DTI

Comparison of FA in the central region (Table 3 and Fig 2*B*) elucidates that group IV (EE probable/definite) mean values reside below the double-SD threshold of healthy controls (group Ib): 356.21 ± 48.50 versus 475.09 ± 50.41 ($P < .001$). Overall, mean FA values of groups III (EE clinically possible) and IV were significantly lower in the upper 3 regions of measurements (Table 3), except for the mean precentral gyrus FA reduction of group III (which also was beyond the 1 SD threshold). In the brain stem regions, the groups resided closely together: There was only 1 larger FA difference in the pons region for group IV ($P = .062$, Table 3).

MD exhibited statistically significant differences with MD elevation in the internal capsule in group IV compared with healthy controls (849.43 ± 54.77 versus 774.44 ± 56.91 [$\times 10^{-6}$ mm^2/s] in controls, $P < .001$).

When averaging FA and MD statistics on the CSTs as a whole, we found no significant differences between single groups (Table 3, $P > .05$). On the other hand, there was a decrease toward groups III and IV regarding the mean amount

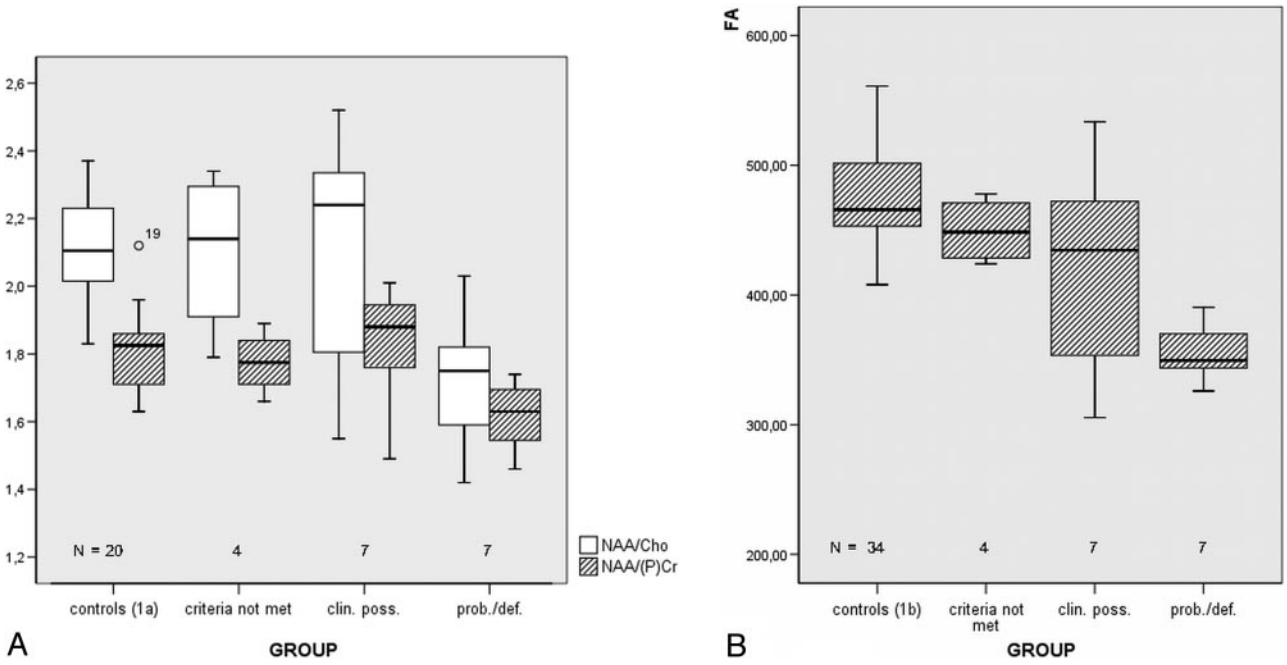

Fig 2. *A,* NAA/Cho and NAA/PCr metabolite ratios for patient subgroups and controls. Both parameters are lowest in group IV (EE probable/definite [prob./def.]). *B,* FA boxplots of the central region for groups I–IV. Mean FA values of groups III (EE clinically possible [clin. poss.]) and IV (prob./def.) were markedly lower in the upper 3 regions of measurements (Table 3).

Table 3: DTI group results and Mann-Whitney–Wilcoxon test for comparison of mean FA with healthy controls (group Ib)*

FA	Pyramid	Pons	Peduncle	Capsule	Cent. Semi.	Precent. Gyr.	FA CST	MD CST
Group IV								
Mean	456.07	489.71	593.93	570.93	426.21	356.21	510.64	901.14
SD	64.98	111.86	62.62	55.01	84.69	48.50	36.10	31.99
MWW		($P = .062$)		($P = .001$)	($P = .001$)	($P < .001$)	($P > .05$)	($P > .05$)
Group III								
Mean	508.71	553.64	617.86	612.64	435.93	417.86	510.71	932.93
SD	71.20	60.87	64.34	30.82	67.28	85.67	13.82	110.01
MWW		($P > .05$)		($P = .022$)	($P < .001$)	($P = .116$)	($P > .05$)	($P > .05$)
Group II								
Mean	498.75	531.00	582.38	643.75	475.75	449.75	525.13	888.63
SD	64.25	45.76	97.70	51.24	63.29	34.02	17.04	50.71
Group Ib (controls)								
Mean	495.32	577.29	592.06	648.34	531.66	475.09	524.25	897.10
SD	63.47	66.97	65.80	48.97	53.97	50.41	24.58	34.92

Note:—MWW indicates Mann-Whitney–Wilcoxon test; Cent. Semi., centrum semiovale; Precent. Gyr., precentral gyrus; DTI, diffusion tensor imaging; FA, fractional anisotropy.
* The lowest mean FA in comparison with controls is found in the internal capsule, centrum semiovale, and the precentral gyrus of group IV (EE clinically probable/definite) and the internal capsule and centrum semiovale for patients of group III (EE clinically possible). The rightmost FA/MD CST columns illustrate diffusion characteristics averaged for the entire CST. FA ranges from 1000 (maximum anisotropy) to 0 (no anisotropy). MD exhibits statistically significant differences with elevation in the internal capsule in group IV compared with healthy controls (data not shown).

of voxels of which the tracked CSTs consisted (controls: 1594.68 ± 795.55; group III: 928.43 ± 422.26, $P = .034$; group IV: 651.36 ± 419.97, $P = .004$).

Follow-Up Examinations

After 6 months, a clinical follow-up assessment was obtained in 12 patients: There was a progression from the clinically probable to EE "definite" state in 1 patient with positive initial DTI and MR spectroscopy results (IV/4, Table 1), whereas 3 patients of the clinically possible group still had no clinical or electrophysiologic evidence of the UMN being affected (III/2, III/5, III/7). Two clinically possible patients received a second MR spectroscopy/DTI analysis with newly marked FA reduction that had not been present in their initial studies. Compared with the initial state, the first patient (III/4) had a 35% relative FA reduction in the pons (which was the maximum of observed changes) and further reduction in the left and right centrum semiovale (below the 2 SD threshold). Correspondingly, this patient newly exhibited a positive Babinski sign and hyperreflexia. The second patient (III/6) had new FA decrease below the 2 SD threshold for 2 adjacent regions of measurement (the precentral gyrus and centrum semiovale), thus becoming "positive" regarding motor neuron disease–defining DTI criteria. Clinically, there was a progression of symptoms in this patient, with a lesion of the central pathways to the right leg in electrophysiology. No newly evolved symptoms could be observed in the other follow-up patients (IV/3, IV/5, IV/6, III/1, III/3, and II/2). Patient III/1 still lacked any LMN signs (thus representing a case of UMN–dominant ALS or PLS) at the time of his follow-up; patient II/2 received an MR imaging follow-up, with negative findings (as were the findings of his initial clinical and MR evaluation).

Synopsis

Clinical assessment, MR spectroscopy, and DTI findings are summarized in Table 1: In patients with clinical evidence for UMN involvement (IV/1-III/1), there was no false-negative case in their MR imaging work-up. In patients without UMN involvement or with different diagnoses (III/2-II/4), there was 1 false-positive diagnosis: DTI and MR spectroscopy findings concurrently were false-positive in 1 patient with lower motor neuron involvement only (patient III/2). Most interesting, a patient with an ex post genetically proved Kennedy syndrome (II/3) exhibited true-negative DTI results and false-positive MR spectroscopy results (with an overall negative result because of divergent findings). With MR spectroscopy and DTI thus concordant at the level of the precentral gyrus and corona radiata in all except 3 patients (III/5, III/7, II/3, Cohen κ = 0.73), sensitivity and specificity were 75% and 80% for MR spectroscopy and 75% and 90% for DTI. Under the assumption of an overall negative result of the MR spectroscopy/DTI combination in the case of divergent findings, MR spectroscopy/DTI sensitivity was 100% and specificity 90%.

Discussion

Whereas anatomic 3T MR imaging signs are by far not sufficient, combined 3T MR spectroscopy and DTI improve diagnostic accuracy in the work-up of patients with suspected motor neuron disease: There was no false-negative case in patients with EE probable or definite assessments. This combination gave further evidence to exclude all patients with suspected motor neuron disease who did not meet EE criteria and to include 2 clinically possible patients (by means of follow-up examinations).

In the subset of patients who lacked UMN signs—which is the clinically most important group—markedly reduced mean FA was found in 3 regions (the internal capsule, the centrum semiovale, and the motor cortex). Progressing FA decline in this group was observed in 2 follow-up examinations. We thus provide data for a patient subgroup with clinical lower motor neuron disease only, which is considered a target group for future ALS studies.[21,45]

Because studies using high-field magnets (≥3T) and applying both spectroscopy and DTI to the same patients with suspected ALS are still rare,[22,23] reviews regarding congruent or incongruent results of both techniques are essential. In the present study, MR spectroscopy and DTI agreement was high: Markedly reduced FA with corresponding NAA reductions occurred in all clinically definite/probable patients with ALS, with a total of only 3 divergent findings. Furthermore, so far FA measurements were confined to a limited number of CST levels only.[21] FA and MD data in our study were collected along the whole CST at levels of the brain stem, the internal capsule, the corona radiata, and the precentral gyrus and revealed changes in several adjacent regions that are complementary to abnormalities detected by the (centrally placed) spectroscopic VOI. We also calculated FA and MD statistics for the tracked CST as whole objects in all patients and controls. Most interesting, this approach yielded no larger FA or MD differences for the entire CST but showed a significant reduction of CST voxels toward the possible and definite groups, as has been indicated by volumetric analyses earlier.[46] It may well be that the results of fiber tracking algorithms in patients with motor neuron disease predominantly reveal unchanged CST remainders, which are consecutively composed of smaller amounts of voxels and throughout which diffusion characteristics are not significantly altered compared with healthy subjects. Macroscopic abnormalities in structural MR images predominantly occur in advanced stages of the disease. Thus, DTI-based CST volumetry or voxel-based morphometry[47] may be able to detect structural changes earlier than it would be possible by relying on visually recognizable anatomic MR imaging signs alone.

It has been a matter of debate whether MD elevation reflects more chronic changes in the disease process of ALS. In this study, significant MD elevation only was observed at the internal capsule for the clinically probable and definite patients. MD differences tend to be lost caudally in the CST[48] and, furthermore, could not be ascertained by other groups.[22] For the motor region and centrum semiovale, it is questionable whether MD changes correlate with disease processes or are not rather due to extracellular volume increases in the course of atrophic changes.

As shown in our previous ALS studies using MR spectroscopy, the NAA/Cho metabolite ratio served as a robust parameter with good discriminatory power for patient subgroups.[8,9] Single-voxel spectroscopy in combination with DTI was used rather than spectroscopic imaging because of its inherent higher signal-intensity-to-noise ratio (96 averages were used as a maximum for our measurements) and the possibility for a reliable absolute quantification of metabolites. However, evaluation with MR spectroscopy alone is inferior to the MR spectroscopy/DTI combination, as is well illustrated by the pathologic MR spectroscopy findings in the patient with Kennedy syndrome (who had normal FA), which could have lead to the erroneous assumption of motor neuron disease (whereas there is a normal average life expectancy in the case of SBMA; pathologic MR spectroscopy findings in Kennedy disease have been reported earlier[49]).

Conclusion

The MR spectroscopy/DTI combination at 3T effectively adds to the detection of motor neuron disease and improves diagnostic confidence.

References

1. Strong M, Rosenfeld J. **Amyotrophic lateral sclerosis: a review of current concepts.** *Amyotroph Lateral Scler Other Motor Neuron Disord* 2003;4:136–43
2. Gordon PH, Cheng B, Katz IB, et al. **The natural history of primary lateral sclerosis.** *Neurology* 2006;66:647–53
3. Urban PP, Wicht S, Hopf HC. **Sensitivity of transcranial magnetic stimulation of cortico-bulbar vs. cortico-spinal tract involvement in Amyotrophic Lateral Sclerosis (ALS).** *J Neurol* 2001;248:850–55
4. Buhler R, Magistris MR, Truffert A, et al. **The triple stimulation technique to study central motor conduction to the lower limbs.** *Clin Neurophysiol* 2001;112:938–49
5. Brooks BR, Miller RG, Swash M, et al. **El Escorial revisited: revised criteria for the diagnosis of amyotrophic lateral sclerosis.** *Amyotroph Lateral Scler Other Motor Neuron Disord* 2000;1:293–99
6. Cedarbaum JM, Stambler N, Malta E, et al. **The ALSFRS-R: a revised ALS functional rating scale that incorporates assessments of respiratory function: BDNF ALS Study Group (Phase III).** *J Neurol Sci* 1999;169:13–21
7. Block W, Karitzky J, Traber F, et al. **Proton magnetic resonance spectroscopy of the primary motor cortex in patients with motor neuron disease: subgroup analysis and follow-up measurements.** *Arch Neurol* 1998;55:931–36
8. Pohl C, Block W, Traber F, et al. **Proton magnetic resonance spectroscopy and transcranial magnetic stimulation for the detection of upper motor neuron degeneration in ALS patients.** *J Neurol Sci* 2001;190:21–27

9. Pohl C, Block W, Karitzky J, et al. **Proton magnetic resonance spectroscopy of the motor cortex in 70 patients with amyotrophic lateral sclerosis.** *Arch Neurol* 2001;58:729–35
10. Ellis CM, Simmons A, Andrews C, et al. **A proton magnetic resonance spectroscopic study in ALS: correlation with clinical findings.** *Neurology* 1998;51:1104–09
11. Kalra S, Cashman NR, Genge A, et al. **Recovery of N-acetylaspartate in corticomotor neurons of patients with ALS after riluzole therapy.** *Neuroreport* 1998;9:1757–61
12. Cosottini M, Giannelli M, Siciliano G, et al. **Diffusion-tensor MR imaging of corticospinal tract in amyotrophic lateral sclerosis and progressive muscular atrophy.** *Radiology* 2005;237:258–64
13. Ellis CM, Simmons A, Jones DK, et al. **Diffusion tensor MRI assesses corticospinal tract damage in ALS.** *Neurology* 1999;53:1051–58
14. Graham JM, Papadakis N, Evans J, et al. **Diffusion tensor imaging for the assessment of upper motor neuron integrity in ALS.** *Neurology* 2004;63:2111–19
15. Hong YH, Lee KW, Sung JJ, et al. **Diffusion tensor MRI as a diagnostic tool of upper motor neuron involvement in amyotrophic lateral sclerosis.** *J Neurol Sci* 2004;227:73–78
16. Jacob S, Finsterbusch J, Weishaupt JH, et al. **Diffusion tensor imaging for long-term follow-up of corticospinal tract degeneration in amyotrophic lateral sclerosis.** *Neuroradiology* 2003;45:598–600
17. Sach M, Winkler G, Glauche V, et al. **Diffusion tensor MRI of early upper motor neuron involvement in amyotrophic lateral sclerosis.** *Brain* 2004;127:340–50
18. Toosy AT, Werring DJ, Orrell RW, et al. **Diffusion tensor imaging detects corticospinal tract involvement at multiple levels in amyotrophic lateral sclerosis.** *J Neurol Neurosurg Psychiatry* 2003;74:1250–57
19. Ulug AM, Grunewald T, Lin MT, et al. **Diffusion tensor imaging in the diagnosis of primary lateral sclerosis.** *J Magn Reson Imaging* 2004;19:34–39
20. Aoki S, Iwata NK, Masutani Y, et al. **Quantitative evaluation of the pyramidal tract segmented by diffusion tensor tractography: feasibility study in patients with amyotrophic lateral sclerosis.** *Radiat Med* 2005;23:195–99
21. Wang S, Poptani H, Woo JH, et al. **Amyotrophic lateral sclerosis: diffusion-tensor and chemical shift MR imaging at 3.0 T.** *Radiology* 2006;239:831–38
22. Yin H, Lim CC, Ma L, et al. **Combined MR spectroscopic imaging and diffusion tensor MRI visualizes corticospinal tract degeneration in amyotrophic lateral sclerosis.** *J Neurol* 2004;251:1249–54
23. Mitsumoto H, Ulug AM, Pullman SL, et al. **Quantitative objective markers for upper and lower motor neuron dysfunction in ALS.** *Neurology* 2007;68:1402–10
24. Chan S, Kaufmann P, Shungu DC, et al. **Amyotrophic lateral sclerosis and primary lateral sclerosis: evidence-based diagnostic evaluation of the upper motor neuron.** *Neuroimaging Clin N Am* 2003;13:307–26
25. Brooks BR. **What are the implications of early diagnosis? Maintaining optimal health as long as possible.** *Neurology* 1999;53:S43–S45
26. Brooks BR. **Earlier is better: the benefits of early diagnosis.** *Neurology* 1999;53:S53–S54
27. Goodin DS, Rowley HA, Olney RK. **Magnetic resonance imaging in amyotrophic lateral sclerosis.** *Ann Neurol* 1988;23:418–20
28. Udaka F, Sawada H, Seriu N, et al. **MRI and SPECT findings in amyotrophic lateral sclerosis: demonstration of upper motor neurone involvement by clinical neuroimaging.** *Neuroradiology* 1992;34:389–93
29. Cheung G, Gawel MJ, Cooper PW, et al. **Amyotrophic lateral sclerosis: correlation of clinical and MR imaging findings.** *Radiology* 1995;194:263–70
30. Hofmann E, Ochs G, Pelzl A, et al. **The corticospinal tract in amyotrophic lateral sclerosis: an MRI study.** *Neuroradiology* 1998;40:71–75
31. Hecht MJ, Fellner F, Fellner C, et al. **MRI-FLAIR images of the head show corticospinal tract alterations in ALS patients more frequently than T2-, T1- and proton-density-weighted images** *J Neurol Sci* 2001;186:37–44
32. Hecht MJ, Fellner F, Fellner C, et al. **Hyperintense and hypointense MRI signals of the precentral gyrus and corticospinal tract in ALS: a follow-up examination including FLAIR images.** *J Neurol Sci* 2002;199:59–65
33. Ishikawa K, Nagura H, Yokota T, et al. **Signal loss in the motor cortex on magnetic resonance images in amyotrophic lateral sclerosis.** *Ann Neurol* 1993;33:218–22
34. Oba H, Araki T, Ohtomo K, et al. **Amyotrophic lateral sclerosis: T2 shortening in motor cortex at MR imaging.** *Radiology* 1993;189:843–46
35. Grosskreutz J, Kaufmann J, Fradrich J, et al. **Widespread sensorimotor and frontal cortical atrophy in amyotrophic lateral sclerosis.** *BMC Neurol* 2006;6:17
36. Young S, Bystrov D, Netsch T, et al. **Automated planning of MRI neuro scans.** In: Reinhardt JM, Pluim JPW, eds. *Medical Imaging 2006: Image Processing.* San Diego, Calif, SPIE Medical Imaging; 2006:6144(1), 61441M-8
37. Naressi A, Couturier C, Devos JM, et al. **Java-based graphical user interface for the MRUI quantitation package.** *MAGMA* 2001;12:141–52
38. Vanhamme L, van den BA, Van HS. **Improved method for accurate and efficient quantification of MRS data with use of prior knowledge.** *J Magn Reson* 1997;129:35–43
39. Träber F, Block W, Lamerichs R, et al. **1H metabolite relaxation times at 3.0 tesla: measurements of T1 and T2 values in normal brain and determination of regional differences in transverse relaxation.** *J Magn Reson Imaging* 2004;19:537–45
40. Jaermann T, Crelier G, Pruessmann KP, et al. **SENSE-DTI at 3 T.** *Magn Reson Med* 2004;51:230–36
41. Mori S, Kaufmann WE, Davatzikos C, et al. **Imaging cortical association tracts in the human brain using diffusion-tensor-based axonal tracking.** *Magn Reson Med* 2002;47:215–23
42. Mori S, Crain BJ, Chacko VP, et al. **Three-dimensional tracking of axonal projections in the brain by magnetic resonance imaging.** *Ann Neurol* 1999;45:265–69
43. Stieltjes B, Kaufmann WE, van Zijl PC, et al. **Diffusion tensor imaging and axonal tracking in the human brainstem.** *Neuroimage* 2001;14:723–35
44. Wakana S, Jiang H, Nagae-Poetscher LM, et al. **Fiber tract-based atlas of human white matter anatomy.** *Radiology* 2004;230:77–87
45. Wang S, Melhem ER. **Amyotrophic lateral sclerosis and primary lateral sclerosis: the role of diffusion tensor imaging and other advanced MR-based techniques as objective upper motor neuron markers.** *Ann N Y Acad Sci* 2005;1064:61–77
46. Wang S, Poptani H, Bilello M, et al. **Diffusion tensor imaging in amyotrophic lateral sclerosis: volumetric analysis of the corticospinal tract.** *AJNR Am J Neuroradiol* 2006;27:1234–38
47. Sage CA, Peeters RR, Gorner A, et al. **Quantitative diffusion tensor imaging in amyotrophic lateral sclerosis.** *Neuroimage* 2007;34:486–99
48. Provenzale J. **Amyotrophic lateral sclerosis (ALS).** In: Osborn AG, ed. *Diagnostic Imaging Brain.* 3rd ed. Salt Lake City, Utah: Amirsys Inc; 2005:I/10:86–90
49. Karitzky J, Block W, Mellies JK, et al. **Proton magnetic resonance spectroscopy in Kennedy syndrome.** *Arch Neurol* 1999;56:1465–71